Enhancement of Gap Junction Function During Acute Myocardial Infarction Modifies Healing and Reduces Late Ventricular Arrhythmia Susceptibility

Fu Siong Ng, MBBS, PhD, Jeremy M. Kalindjian, MBBS, Simon A. Cooper, MBBS, Rasheda A. Chowdhury, PhD, Pravina M. Patel, BSc, Emmanuel Dupont, PhD, Alexander R. Lyon, BMBCh, PhD, Nicholas S. Peters, MBBS, MD.

Imperial College London, UK

Funding:
Medical Research Council (Clinical Research Training Fellowship G0900396 to FSN) and the British Heart Foundation (Programme Grant RG/10/11/28457 to NSP and Intermediate Research Fellowship FS/11/67/28954 to ARL).
No conflicts of interest or relationships relevant to this paper.

Correspondence:
Fu Siong Ng
4th Floor, ICTEM Building,
Imperial College London,
Du Cane Road, London W12 0NN, UK.
E-mail: f.ng@imperial.ac.uk
Tel:+442075943614
Fax:+442033122291

Words: 4500

Abstract

Objectives: To investigate the effects of enhancing gap junction (GJ) coupling during acute myocardial infarction (MI) on the healed infarct scar morphology and late post-MI arrhythmia susceptibility.

Background: Increased heterogeneity of myocardial scarring after MI is associated with greater arrhythmia susceptibility. We hypothesized that short-term enhancement of GJ coupling during acute MI can produce more homogeneous infarct scars, reducing late susceptibility to post-MI arrhythmias.

Methods: Following arrhythmic characterisation of the rat 4-week post-MI model (n=24), a further 27 Sprague-Dawley rats were randomised to receive rotigaptide to enhance GJ coupling (n=13) or saline control (n=14) by osmotic minipump immediately prior to, and for the first 7 days following surgical MI. At 4 weeks post-MI, hearts were explanted for *ex vivo* programmed electrical stimulation (PES) and optical mapping. Heterogeneity of infarct border zone (IBZ) scarring was quantified by histomorphometry.

Results: Despite no detectable difference in infarct size at 4 weeks post-MI, rotigaptide-treated hearts had reduced arrhythmia susceptibility during PES (Inducibility score: rotigaptide 2.4±0.8, control 5.0±0.6, p=0.02) and less heterogeneous IBZ scarring (standard deviation of IBZ Complexity Score: rotigaptide 1.1±0.1, control 1.4±0.1, p=0.04), associated with an improvement in IBZ conduction velocity (rotigaptide 43.1±3.4 cm/s, control 34.8±2.0 cm/s, p=0.04).

Conclusions: Enhancement of GJ coupling for only 7 days at the time of acute MI produced more homogeneous IBZ scarring and reduced arrhythmia susceptibility at 4 weeks post-MI. Short-term GJ modulation at the time of MI may represent a novel treatment strategy to modify the healed infarct scar morphology and reduce late post-MI arrhythmic risk.

Key words: Ventricular arrhythmias, myocardial infarction, gap junctions, electrophysiology, fibrosis

Condensed abstract

Increased heterogeneity of myocardial scarring after myocardial infarction (MI) is associated with greater arrhythmia susceptibility. We demonstrate that short-term treatment with rotigaptide, a pharmacological gap junction enhancer, immediately before, and for seven days only during acute MI can modify the morphology of the healed infarct scar at four weeks post-MI. Rotigaptide-treated hearts had more homogeneous infarct scars, associated with an increase in infarct border zone conduction velocity and a reduction in arrhythmia susceptibility during programmed electrical stimulation. Short-term gap junction modulation at the time of MI may represent a novel treatment strategy to reduce late post-MI arrhythmic risk.

Abbreviations

MI: Myocardial infarction

GJ: Gap junction

IBZ: Infarct border zone

PES: Programmed electrical stimulation

Cx43: connexin43

CV: Conduction velocity

APD: Action potential duration

VT: Ventricular tachycardia

Introduction

Ventricular arrhythmias are responsible for the majority of the 300,000 annual sudden cardiac deaths in the USA (1), with myocardial infarction (MI) being the principal underlying cause. Many sudden deaths in patients with MI occur months to years after their index event. Heterogeneity of infarct scarring has been identified as a determinant of late post-MI arrhythmias, with increased heterogeneity of fibrosis being associated with increased arrhythmic risk (1-3). In the infarct border zone (IBZ), heterogeneous scarring produces bundles of surviving myocardium within areas of dense fibrotic scar creating the substrate for re-entrant circuits causing late post-MI VT (4-6). Therapeutic strategies to homogenise infarct scar, both by ablation or pharmacologically, have been shown to be anti-arrhythmic in the chronically infarcted heart (7-9).

Gap junctions (GJs) are clusters of transmembrane channels that mediate coupling of the cytoplasmic compartments of adjacent cells, and allow cell-to-cell transfer of ions and small molecules. Studies have shown that modulating GJ coupling can modify the intercellular passage of products of cell necrosis, affect infarct spread and may have small effects on the size of the healed infarct (10-12). Enhancing GJ coupling during MI, at a time when natural GJ uncoupling occurs (13), would be expected to increase gap junctional exchange of chemical mediators of cell death and survival between healthy and dying cells at the ischaemic border, thus homogenising the distribution of cell death and survival during MI. Although any resulting myocardial salvage may be inadequate to significantly alter myocardial mechanical function, even subtle alterations of the morphology of the scar border relating to increased homogeneity of scarring in the healed infarct may have important effects on late post-MI arrhythmia susceptibility.

We hypothesized that enhancing GJ coupling for a limited duration only, at the time of MI, can reduce late arrhythmia susceptibility in a chronically infarcted heart, resulting from greater

homogeneity of scarring in the healed infarct. We characterised the arrhythmic behaviour and electrophysiology in a rat model of healed MI, and investigated the effects of short-term GJ enhancement during acute MI on the morphology and arrhythmia susceptibility of the healed infarct scar.

Methods

The methods are briefly described here. For full details, please see the **Supplementary Materials**.

Ethical approval

This work was performed in accordance with standards set out in the United Kingdom Animals (Scientific Procedures) Act 1986, and was approved by the Imperial College London Ethical Review Board and carried out under Project License PPL 70/7033.

Experimental protocols

In order to characterise the arrhythmic behaviour and electrophysiology of our 4-week chronic MI model, 24 male Sprague-Dawley rats (250g-300g) were subjected to surgical MI by left anterior descending (LAD) artery ligation as previously described (14), while four rats underwent sham MI surgery. After four weeks healing, rats were sacrificed and hearts were explanted, perfused *ex vivo*, subjected to optical mapping of transmembrane voltage as previously described (15), and to programmed electrical stimulation (PES) to provoke ventricular arrhythmias.

To assess the effects of short-term GJ modulation during acute MI on the healed infarct morphology and arrhythmia susceptibility at the chronic healed MI phase, another 27 rats were randomly allocated to one of 2 groups receiving 7 days of either: (1) rotigaptide to enhance GJ coupling (n=13), or (2) phosphate-buffered saline (PBS) as the control group (n=14). We had previously confirmed that rotigaptide enhances GJ coupling in ventricular myocardium in the context of acute ischaemia/metabolic stress in separate immunoblotting and *ex vivo* optical mapping experiments described in the **Supplementary Results**, consistent with previous studies in the literature (16).

Animals were given a bolus of GJ modulator or vehicle subcutaneously immediately before LAD ligation (2.5nmol/kg rotigaptide or 0.5ml PBS). GJ modulator or vehicle was then delivered for the first 7 days post-MI using intraperitoneal osmotic minipumps (infusion rate: rotigaptide 0.11nmol/kg/min, or PBS 2ml/week) (10). At four weeks post-MI (i.e. 3 weeks after discontinuation of rotigaptide administration), hearts were explanted for *ex vivo* optical mapping with arrhythmia provocation studies (PES). The vulnerability of hearts to PES-induced arrhythmias was quantified using a previously described and validated Arrhythmia Inducibility Score for PES in rat hearts (17). Hearts were then frozen and sectioned for histological staining with Masson's trichrome, for maximum contrast and differentiation between scar and surviving myocardium, and for Cx43 immunolabeling.

Histology and histomorphometry

Infarct size was quantified by planimetry using previously validated methods (18, 19). Briefly, the endocardial and epicardial circumferences of the infarct were measured for each section, and the infarct size quantified as the proportion of the endocardial and epicardial circumferences bounded by the transmural infarct.

The complexity of IBZ scarring and the degree of heterogeneity of fibrosis was quantified using an Interface Complexity Ratio (ICR), defined as the ratio of the length of interface between fibrosis and surviving myocardium to the area of fibrosis in that microscopic field (see **Supplementary Methods** and **Supplemental Figure 2**). IBZs with greater heterogeneity of fibrosis have greater ratios, i.e. greater interface between fibrotic and myocardial tissue per unit area of fibrosis. The inter-observer and intra-observer coefficients of variation for this method were 12% and 10% respectively. For each heart, 10µm slices were taken at 500µm intervals across the entire infarct for staining, with 27±5 IBZ microscopic fields analysed per slice. The ICR values were then averaged to give a single mean

value and a single standard deviation value, as a measure of dispersion, per heart. All experiments and analyses were performed blinded to treatment group.

Data analysis and statistics

Optical mapping data were analysed as previously described (15, 20, 21). Activation maps were generated, and local conduction velocities and vectors were derived, using MATLAB R2010a software (MathWorks, Massachusetts, USA). Analysis of variance (ANOVA) tests were performed to compare means between multiple groups and post-hoc Tukey's test was used if ANOVA was significant. Student's T-tests were used to compare means between two groups. A p-value of <0.05 was considered significant. All values shown are mean ± S.E.M.

Results

Characterisation of conduction, optical action potentials, and arrhythmogenesis in the chronic healed MI model

Sixteen of 24 (66%) infarcted rats, and all 4 sham-operated rats, survived the acute surgery. Optical mapping studies were performed at 4 weeks post-MI. **Figure 1A** shows representative activation maps and local conduction velocity (CV) maps for a chronically infarcted heart, and **Figure 1B** shows representative optical action potentials from the remote non-infarcted myocardium, the IBZ and the infarct zone. There was a 47% reduction in IBZ CV compared to remote non-infarcted myocardium (34.1±3.2 cm/s vs. 67.6±3.8 cm/s, $p<0.0001$; **Figure 1C**). CVs in the remote myocardium of MI hearts were not different from the same myocardial region of sham-operated hearts (73.4±5.8 cm/s). There was increased dispersion of conduction vector angles in the infarct zone compared to the IBZ and remote myocardium, demonstrating greater heterogeneity in directions of activation within the infarct (**Figure 1D**).

Optical action potential (AP) rise times in the infarct zone and IBZ were prolonged compared with those recorded at the remote, viable myocardium and those from sham-operated hearts (**Figures 1E**). Mean action potential durations (APDs) were not different between the infarct zone, IBZ and remote myocardium, but there was greater spatial variability of APDs in the infarct zone and IBZ compared to remote myocardium and to sham-operated hearts (**Figure 1F**).

Hearts were classified for arrhythmia susceptibility based on the PES experiments, and were ranked for arrhythmia susceptibility and then divided into two groups based on the median values. Hearts in the more arrhythmic (+) group had values above the median and hearts in the less arrhythmic (-) group had values below the median. As shown in **Figure 1G**, IBZ CVs were significantly slower in

the PES(+) hearts compared to the PES(-) hearts (27.6 ± 3.8 cm/s vs. 39.3 ± 4.1 cm/s, p=0.04), suggesting that IBZ CV is a determinant of susceptibility to ventricular arrhythmias on PES in chronic MI hearts.

Effects of rotigaptide treatment on conduction, optical action potentials and arrhythmogenesis in healed MI

Of animals randomised to treatment with either rotigaptide (n=13) or control (n=14), 9 animals from the rotigaptide group and 10 from the control group survived acute MI surgery (acute mortality: rotigaptide 31%, control 29%, p=NS). At four weeks post-MI, hearts of animals treated with rotigaptide for the first 7 days post-MI had reduced arrhythmia inducibility at PES compared to control, with VT/VF induced in fewer rotigaptide-treated hearts for any given number of extrastimuli (**Figure 2A & 2B**) and a reduction in the Arrhythmia Inducibility Score (rotigaptide 2.4±0.8, control 5.0±0.6, p=0.02) (**Figure 2C**). These findings indicate a difference in substrate in rotigaptide hearts compared to control, which rendered hearts more resistant to PES-induced ventricular arrhythmias.

Figure 3A shows representative activation maps and optical APs for control and rotigaptide hearts. Consistent with the demonstration that IBZ CV is a determinant of arrhythmia susceptibility, there was a 24% increase in IBZ CV in rotigaptide-treated hearts compared with untreated post-MI animals (rotigaptide 43.1 ± 3.4 cm/s, control 34.8 ± 2.0, p=0.04) (**Figure 3B**). There were no differences in the optical action potential rise times and durations between groups (**Figure 3C** & **Figure 3D**).

Rotigaptide treatment did not alter infarct size

Surgical LAD artery ligation produced transmural infarcts with compensatory hypertrophy of non-infarcted myocardium, as shown on Masson's Trichrome-stained biventricular sections in **Figure**

4A. Infarct size by planimetry was not different between groups (control 21.0% ± 3.6%, rotigaptide 20.5% ± 1.7%; p=NS) (**Figure 4B**), suggesting that acute GJ enhancement during MI did not grossly alter infarct size and this could not account for the reduced susceptibility to PES-arrhythmias in rotigaptide hearts.

Rotigaptide reduced heterogeneity of fibrosis at the IBZ

Differences in IBZ morphology and structural heterogeneity were determined using the Interface Complexity Ratio, a measure of fibrosis complexity at the IBZ, with greater ratios representing more complex morphologies (see **Supplementary Materials**). **Figure 4C** shows sample images of IBZ from control and rotigaptide hearts. Although the mean Interface Complexity Ratios were not significantly different between groups (control 3.2±0.2, rotigaptide 3.3±0.2, p=NS, **Figure 4D**), the degree of heterogeneity of IBZ scarring was reduced after rotigaptide treatment (standard deviation of Interface Complexity Ratios within each heart: control 1.4±0.1, rotigaptide 1.1±0.1, p=0.04) (**Figure 4E**). The reduction in ICR variability within each heart for the rotigaptide group points towards more homogeneous patterns of IBZ scarring, whereas control hearts exhibited a greater range of IBZ scar morphologies within each heart.

Rotigaptide did not alter post-MI Cx43 maldistribution

There were no differences in mean Cx43 lateralization scores between treatment groups (control 1.3±0.1, rotigaptide 1.3±0.1, p=NS; **Figure 4G**), or in the variability of the Cx43 lateralization scores (standard deviation of Cx43 lateralization score: control 0.5±0.1, rotigaptide 0.5±0.1, p=NS).

Discussion

The principal and important finding of this study is the proof of concept of a highly novel antiarrhythmic strategy of modifying infarct healing by short-term enhancement of GJ function during acute MI, which modifies the healed arrhythmogenic substrate by reducing inhomogeneities of fibrosis at the healed IBZ without gross changes in infarct size, thus reducing VT/VF inducibility late post-MI. The homogenisation of scarring was associated with a corresponding improvement in macroscopic CV across the IBZ.

It is important to emphasize the distinction from previous GJ enhancement studies focused on the direct acute electrophysiological effects of rotigaptide on conduction (22), rather than this paradigm shift of modifying the molecular biology of the disease process itself with an enduring antiarrhythmic effect on infarct scar morphology and a reduction in arrhythmia susceptibility three weeks after discontinuation of rotigaptide.

Enhancement of GJ coupling reduced heterogeneity of scarring and fibrosis at the healed IBZ

GJ channels are known to mediate the spread of small molecules of <1kDa in molecular weight, including the passage of mediators of cell death and cell survival during MI (23). During acute MI, closure of GJ channels occurs (13), thus preventing the passage of these molecules between cells and enhancing differential survival between adjacent cells and clusters of cells because of the heterogeneities in local vascular supply, coronary blood flow and cellular metabolism (24, 25), thus leading to heterogeneous cell death. In keeping with this concept, our principal histomorphological finding of homogenisation of scarring at the IBZ with short-term rotigaptide treatment, as supported by the reduced dispersion of ICR values for each heart, is consistent with possible enhanced gap-junctional exchange of chemical mediators of cell death and survival between healthy and dying

cells of the IBZ resulting in more homogeneous patterns of cell death and infarction (23) (**Supplementary Figure 6**). Potential mediators of cell death that can pass through GJ channels include Ca^{2+}, inositol triphosphate (IP3), cyclic AMP and cyclic GMP (26), whereas potential "rescue messengers" that can protect from cell death include ascorbic acid, reduced glutathione, glucose and ATP (27).

Enhancement of GJ coupling during acute MI reduced late post-MI arrhythmia susceptibility

The reduction in heterogeneity of patterns of fibrosis and scarring at the healed IBZ of the rotigaptide-treated hearts was associated with a reduction in susceptibility to ventricular arrhythmias on PES at 4 weeks post-MI. The observed reduction in heterogeneity of IBZ scarring would be expected to reduce the occurrence of adjacent areas of fast and slow conduction, and therefore reduce the likelihood of arrhythmias.

Our finding is consistent with delayed-enhancement MRI imaging studies, which have found that increased scar heterogeneity correlated strongly with inducibility of monomorphic VT (2), and predicted post-MI mortality (3), with the zones of greatest tissue heterogeneity shown to contain critical isthmus sites of scar-related VT (28). Our proposed strategy of reducing IBZ scar heterogeneity parallels the interventional approach of substrate modification by catheter ablation, which has the effect of homogenizing the infarct scar, thereby reducing or abolishing overall arrhythmia burden (7, 9). Recent clinical studies have demonstrated that extensive ablation via a combined endocardial and epicardial approach to homogenize infarct scars can improve freedom from arrhythmias (7), whilst a similar but less extensive ablation approach of homogenizing scar by ablating conducting channels has also been shown to reduce VT recurrence (9). Our strategy is also supported by recent experiments demonstrating that the homogenization of ventricular scar by the application of collagenase can create a less arrhythmic substrate (8).

Improvement in conduction velocity at the healed IBZ of rotigaptide-treated hearts

The improvement in macroscopic CV across the IBZ in rotigaptide-treated hearts is consistent with the finding of reduced scar heterogeneity in those hearts, which would be expected to reduce the tortuosity and conduction path lengths across the IBZ as described above (5). These findings further support a central role for the IBZ in post-MI arrhythmias and lend further weight to the notion that treatments that alter IBZ scar morphology can alter post-MI arrhythmia susceptibility.

Rotigaptide did not significantly alter infarct size

There were no gross differences in infarct size between control and rotigaptide. Previous studies looking specifically at the effects of GJ enhancement on infarct size have produced conflicting results, with one study demonstrating a minor increase in infarct size (11), whilst studies using pharmacological GJ modulators rotigaptide and danegaptide have shown minor reductions in infarct size (10, 12). These disparities may reflect differences in animal models and of timing and duration of enhancement of coupling, as well as differences in methods of measuring infarct size. In any case, any differences in scar size are at most minimal, and although too small to significantly salvage mechanical contractile function, our findings indicate that even the subtle scar homogenization significantly reduces arrhythmogenesis with the potential for clinical impact.

Study Limitation

Optical recordings of transmembrane potential were limited to a depth of several cells at the subepicardium, which meant we were unable to precisely map the location of re-entrant circuits of the induced arrhythmias, and had to extrapolate the electrophysiology of deeper myocardial layers from subepicardial data, though the use of optical mapping to interrogate the electrophysiology of the IBZ has previously been validated (29).

Although not possible to measure directly the effects of rotigaptide on GJ coupling during acute MI in the *in vivo* cohort, we confirmed in parallel *ex vivo* studies that rotigaptide has the expected effects on conduction velocity and Cx43 phosphorylation consistent with GJ enhancement in acute ischaemia and acute metabolic stress (**Supplementary Materials**).

Conclusions

Enhancement of GJ coupling for a limited duration only during the acute phase of MI can reduce inhomogeneities of fibrosis in the healed IBZ whilst reducing late susceptibility to PES-induced ventricular tachyarrhythmias at the chronic healed infarct phase, and may represent a novel clinically-applicable therapeutic strategy to reduce late post-MI ventricular arrhythmias.

Perspectives

Clinical Competencies: Increased heterogeneity of myocardial scarring after MI is associated with greater arrhythmia susceptibility. Approaches to homogenise scar, such as ablation, have demonstrated anti-arrhythmic benefit. Here, we propose a novel pharmacological strategy to homogenise scar by peri-MI GJ enhancement.

Translational Outlook: Enhancement of GJ coupling during acute MI may represent a novel, clinically-applicable therapeutic strategy to reduce heterogeneities of scarring at the IBZ and reduce post-MI ventricular arrhythmias. In our proof-of-concept study, a loading dose of rotigaptide was administered immediately pre-MI to allow for therapeutic concentrations at the time of MI. Further experiments are required to determine if short-term GJ enhancement commencing after MI onset or chronic GJ enhancement pre-MI confer similar beneficial effects before moving into clinical trials. Furthermore, studies to determine the safety and side-effect profile of limited-duration and chronic GJ enhancement in humans are also required prior to clinical translation.

Acknowledgements

The authors would like to thank the Imperial Drug Discovery Centre for synthesizing the rotigaptide.

References

1. Zheng Z, Croft J, Giles W, Mensah G. Sudden cardiac death in the United States, 1989 to 1998. Circulation 2001;104:2158–2163.

2. Schmidt A, Azevedo CF, Cheng A, et al. Infarct Tissue Heterogeneity by Magnetic Resonance Imaging Identifies Enhanced Cardiac Arrhythmia Susceptibility in Patients With Left Ventricular Dysfunction. Circulation 2007;115:2006–2014.

3. Yan AT, Shayne AJ, Brown KA, et al. Characterization of the peri-infarct zone by contrast-enhanced cardiac magnetic resonance imaging is a powerful predictor of post-myocardial infarction mortality. Circulation 2006;114:32–39.

4. de Bakker J, van Capelle F, Janse M, et al. Reentry as a cause of ventricular tachycardia in patients with chronic ischemic heart disease: electrophysiologic and anatomic correlation. Circulation 1988;77:589–606.

5. de Bakker J, van Capelle F, Janse M, et al. Slow conduction in the infarcted human heart. "Zigzag" course of activation. Circulation 1993;88:915–926.

6. Peters NS, Coromilas J, Severs NJ, Wit AL. Disturbed connexin43 gap junction distribution correlates with the location of reentrant circuits in the epicardial border zone of healing canine infarcts that cause ventricular tachycardia. Circulation 1997;95:988–996.

7. Di Biase L, Santangeli P, Burkhardt DJ, et al. Endo-Epicardial Homogenization of the Scar Versus Limited Substrate Ablation for the Treatment of Electrical Storms in Patients With Ischemic Cardiomyopathy. J Am Coll Cardiol 2012;60:132–141.

8. Yagishita D, Ajijola OA, Vaseghi M, et al. Electrical homogenization of ventricular scar by application of collagenase: a novel strategy for arrhythmia therapy. Circ Arrhythm Electrophysiol 2013;6:776–783.

9. Berruezo A, Fernández-Armenta J, Andreu D, et al. Scar dechanneling: new method for scar-related left ventricular tachycardia substrate ablation. Circ Arrhythm Electrophysiol 2015;8:326–336.

10. Haugan K, Marcussen N, Kjolbye A, Nielsen M, Hennan J, Petersen J. Treatment with the gap junction modifier rotigaptide (ZP123) reduces infarct size in rats with chronic myocardial infarction. J Cardiovasc Pharmacol 2006;47:236–242.

11. Prestia KA, Sosunov EA, Anyukhovsky EP, et al. Increased Cell-Cell Coupling Increases Infarct Size and Does not Decrease Incidence of Ventricular Tachycardia in Mice. Front Physiol 2011;2:1–7.

12. Skyschally A, Walter B, Schultz Hansen R, Heusch G. The antiarrhythmic dipeptide ZP1609 (danegaptide) when given at reperfusion reduces myocardial infarct size in pigs. Naunyn Schmiedebergs Arch Pharmacol 2013;386:383–391.

13. de Groot J, Coronel R. Acute ischemia-induced gap junctional uncoupling and arrhythmogenesis. Cardiovasc Res 2004;62:323–334.

14. Lyon AR, Macleod KT, Zhang Y, et al. Loss of T-tubules and other changes to surface topography in ventricular myocytes from failing human and rat heart. Proc Natl Acad Sci USA

2009;106:6854–6859.

15. Ng FS, Shadi IT, Peters NS, Lyon AR. Selective heart rate reduction with ivabradine slows ischaemia-induced electrophysiological changes and reduces ischaemia-reperfusion-induced ventricular arrhythmias. J Mol Cell Cardiol 2013;59:67–75.

16. Eloff B, Gilat E, Wan X, Rosenbaum D. Pharmacological modulation of cardiac gap junctions to enhance cardiac conduction: evidence supporting a novel target for antiarrhythmic therapy. Circulation 2003;108:3157–3163.

17. Belichard P, Savard P, Cardinal R, et al. Markedly different effects on ventricular remodeling result in a decrease in inducibility of ventricular arrhythmias. J Am Coll Cardiol 1994;23:505–513.

18. Pfeffer J, Pfeffer M, Fletcher P, Braunwald E. Progressive ventricular remodeling in rat with myocardial infarction. Am J Physiol 1991;260:H1406–14.

19. Pfeffer M, Pfeffer J, Steinberg C, Finn P. Survival after an experimental myocardial infarction: beneficial effects of long-term therapy with captopril. Circulation 1985;72:406–412.

20. Ng FS, Holzem KM, Koppel AC, et al. Adverse remodeling of the electrophysiological response to ischemia-reperfusion in human heart failure is associated with remodeling of metabolic gene expression. Circ Arrhythm Electrophysiol 2014;7:875–882.

21. Laughner JI, Ng FS, Sulkin MS, Arthur RM, Efimov IR. Processing and analysis of cardiac optical mapping data obtained with potentiometric dyes. Am J Physiol Heart Circ Physiol 2012;303:H753–H765.

22. Xing D, Kjolbye A, Nielsen M, et al. ZP123 increases gap junctional conductance and prevents reentrant ventricular tachycardia during myocardial ischemia in open chest dogs. J Cardiovasc Electrophysiol 2003;14:510–520.

23. Andrade-Rozental AF, Rozental R, Hopperstad MG, Wu JK, Vrionis FD, Spray DC. Gap junctions: the "kiss of death" and the "kiss of life". Brain Res Brain Res Rev 2000;32:308–315.

24. Ghaleh B, Shen YT, Vatner SF. Spatial heterogeneity of myocardial blood flow presages salvage versus necrosis with coronary artery reperfusion in conscious baboons. Circulation 1996;94:2210–2215.

25. Decking UK, Schrader J. Spatial heterogeneity of myocardial perfusion and metabolism. Basic Res Cardiol 1998;93:439–445.

26. Decrock E, Vinken M, Bol M, et al. Calcium and connexin-based intercellular communication, a deadly catch? Cell Calcium 2011;50:310–321.

27. Decrock E, Vinken M, de Vuyst E, et al. Connexin-related signaling in cell death: to live or let die? Cell Death and Differentiation 2009;16:524–536.

28. Estner HL, Zviman MM, Herzka D, et al. The critical isthmus sites of ischemic ventricular tachycardia are in zones of tissue heterogeneity, visualized by magnetic resonance imaging. Heart Rhythm 2011;8:1942–1949.

29. Ding C, Gepstein L, Nguyen DT, et al. High-resolution optical mapping of ventricular

tachycardia in rats with chronic myocardial infarction. Pacing Clin Electrophysiol 2010;33:687–695.

Figure legends:

Figure 1: Electrophysiology and Arrhythmia Determinants of Chronic MI Model: (A) Optical mapping of chronic MI hearts. (B) Representative optical APs from remote myocardium, IBZ and infarct zone. (C) Slower CVs at IBZ compared with remote myocardium. (D) Conduction vector angles were more heterogeneous in the infarct zone (MI). (E) Prolonged rise times at the infarct zone and IBZ. (F) Increased dispersion of optical APDs at the infarct zone and IBZ. For Figures 1C to 1F, n=16 for MI hearts, and n=4 for sham hearts. (G) IBZ CV was slower in PES(+) hearts (n=8) compared to PES(-) hearts (n=8). (*$p<0.05$, **$p<0.01$, ***$p<0.001$).

Figure 2: Reduced arrhythmia susceptibility on PES in rotigaptide-treated hearts at 4 weeks post-MI. (A) *Top:* Example of VT/VF induced in a control heart during PES. *Bottom:* Example of PES in a rotigaptide heart, with no arrhythmias induced with 3 extrastimuli. (B) Proportions of hearts with VT/VF (duration >1 second) induced with PES (+ve: PES positive, -ve: PES negative. (C) Reduced Arrhythmia Inducibility Scores for rotigaptide hearts (n=9) compared to control MI hearts (n=10) (*$p<0.05$). Data from sham-operated hearts (n=4) presented for comparison.

Figure 3: Improvement in IBZ conduction velocity in rotigaptide-treated hearts. (A) Representative activation maps showing conduction slowing at the IBZ of control and rotigaptide hearts, and representative IBZ optical APs. (B) Increase in IBZ CV in rotigaptide-treated hearts (n=9), when compared with untreated control hearts (n=26). (C&D) No difference in optical AP rise times and AP duration between groups.

Figure 4: Reduced heterogeneity of fibrosis at IBZ of rotigaptide-treated hearts. (A) Representative biventricular slices from the mid-ventricles of MI hearts stained with Masson's Trichrome. (B) No difference in infarct size between groups. (C) Sample images of the IBZ from

control and rotigaptide hearts showing complex interaction between fibrosis (blue) and surviving myocardium (red-pink). (D) Mean IBZ Interface Complexity Ratios (ICRs) were not different between groups. (E) Rotigaptide reduced the dispersion (standard deviation) of ICR compared to control MI hearts (*$p<0.05$). (F) Cx43 lateralization scoring system. *Left:* Normal Cx43 localisation at the intercalated discs. Right: Significant lateralization of Cx43 as shown by arrows. (G) Cx43 lateralization scores were not different between groups. For Figure 4, CON n=10, ROT n=9.

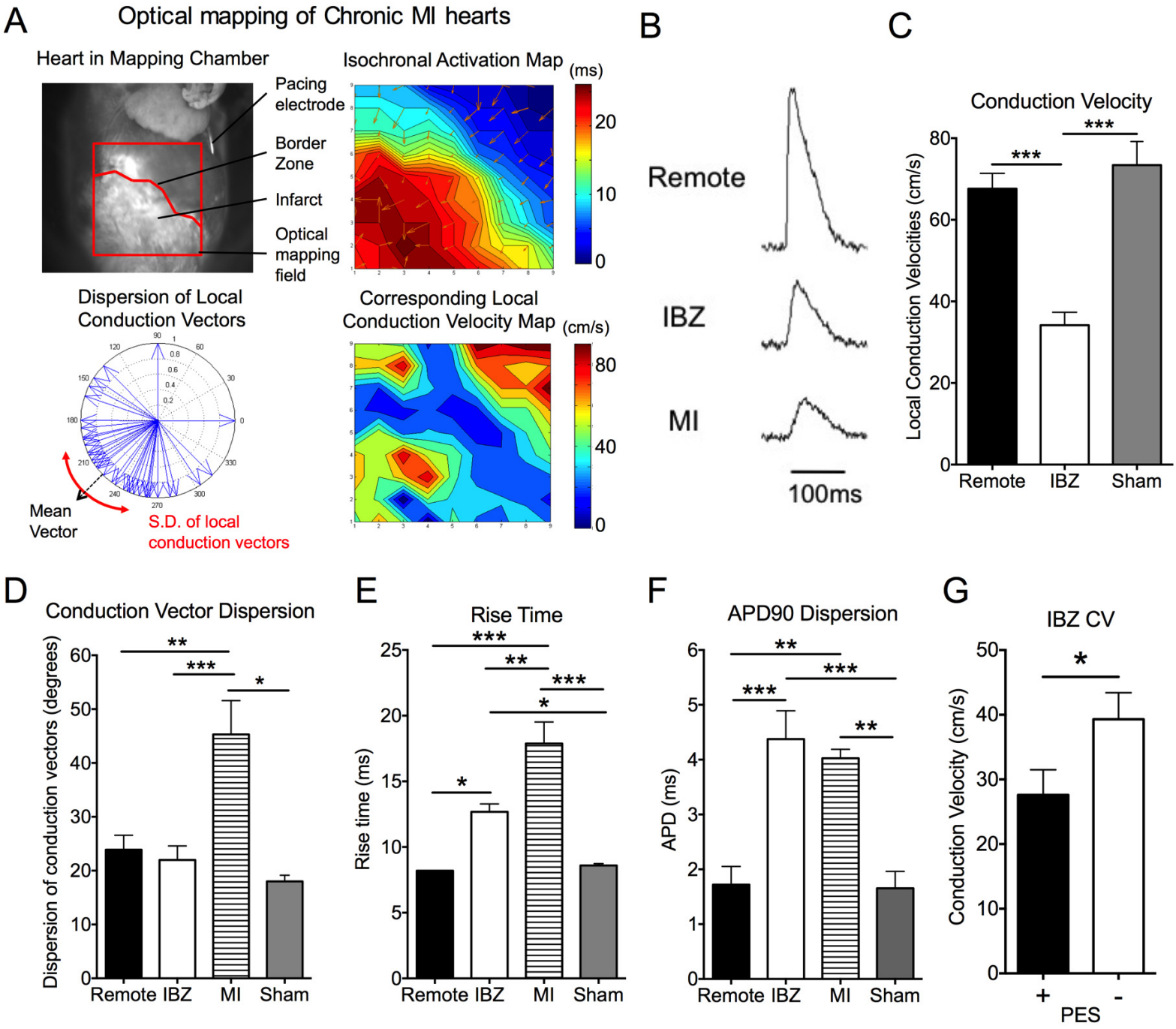
A
Optical mapping of Chronic MI hearts
Heart in Mapping Chamber
Pacing electrode
Border Zone
Infarct
Optical mapping field
Isochronal Activation Map
(ms)
20
10
0
Dispersion of Local Conduction Vectors
Mean Vector
S.D. of local conduction vectors
Corresponding Local Conduction Velocity Map
(cm/s)
80
40
0
B
Remote
IBZ
MI
100ms
C
Conduction Velocity
Local Conduction Velocities (cm/s)
***
***
Remote
IBZ
Sham
D
Conduction Vector Dispersion
Dispersion of conduction vectors (degrees)
**
***
*
Remote
IBZ
MI
Sham
E
Rise Time
Rise time (ms)
***
**
***
*
*
Remote
IBZ
MI
Sham
F
APD90 Dispersion
APD (ms)
**
***
***
**
Remote
IBZ
MI
Sham
G
IBZ CV
Conduction Velocity (cm/s)
*
+
-
PES

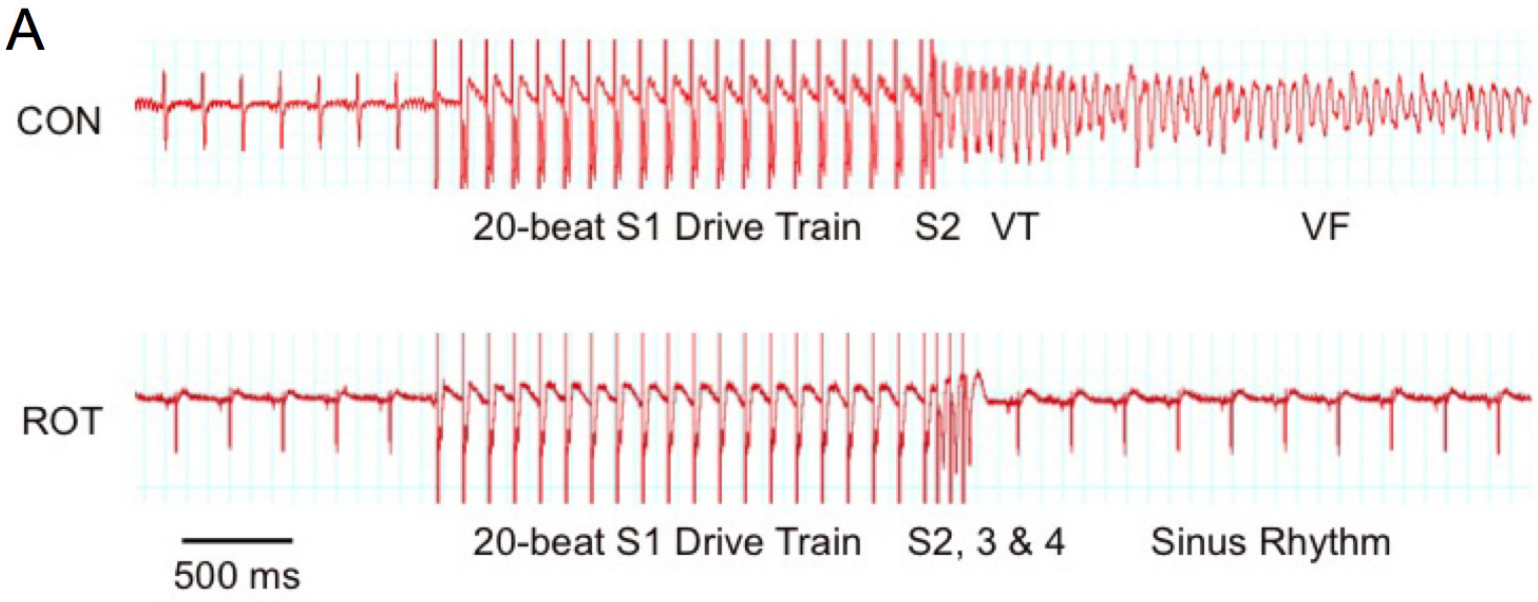
A
CON
20-beat S1 Drive Train
S2
VT
VF
ROT
20-beat S1 Drive Train
S2, 3 & 4
Sinus Rhythm
500 ms

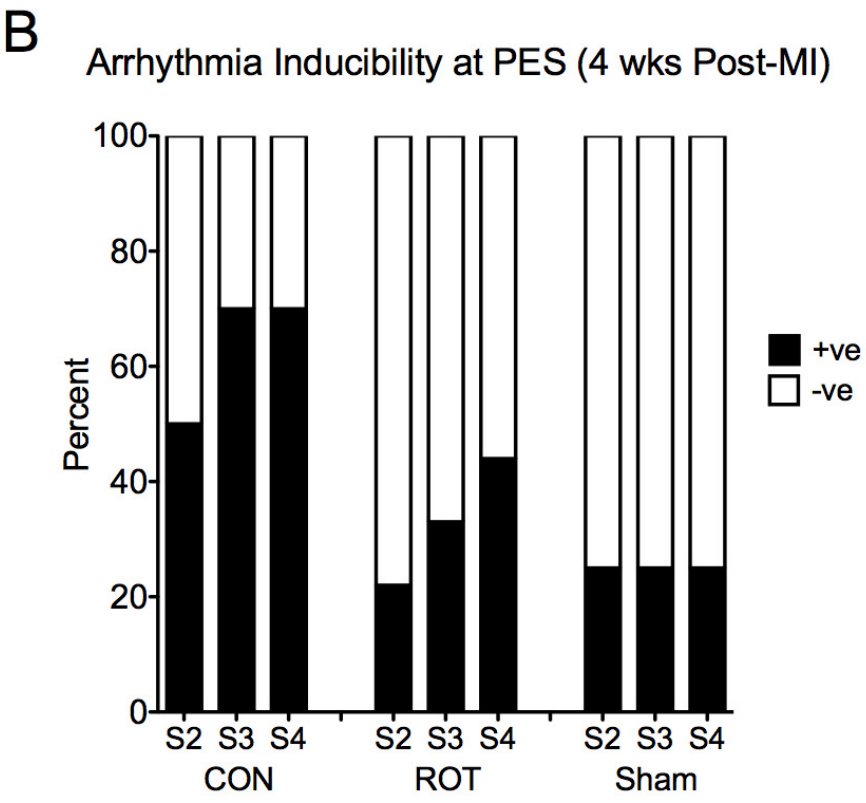
B
Arrhythmia Inducibility at PES (4 wks Post-MI)
Percent
100
80
60
40
20
0
S2 S3 S4
CON
S2 S3 S4
ROT
S2 S3 S4
Sham
+ve
-ve

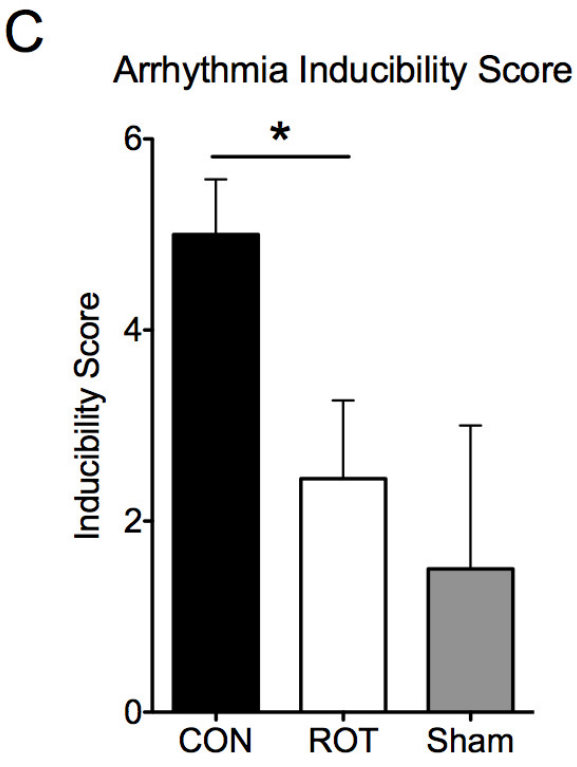
C
Arrhythmia Inducibility Score
*
Inducibility Score
6
4
2
0
CON
ROT
Sham

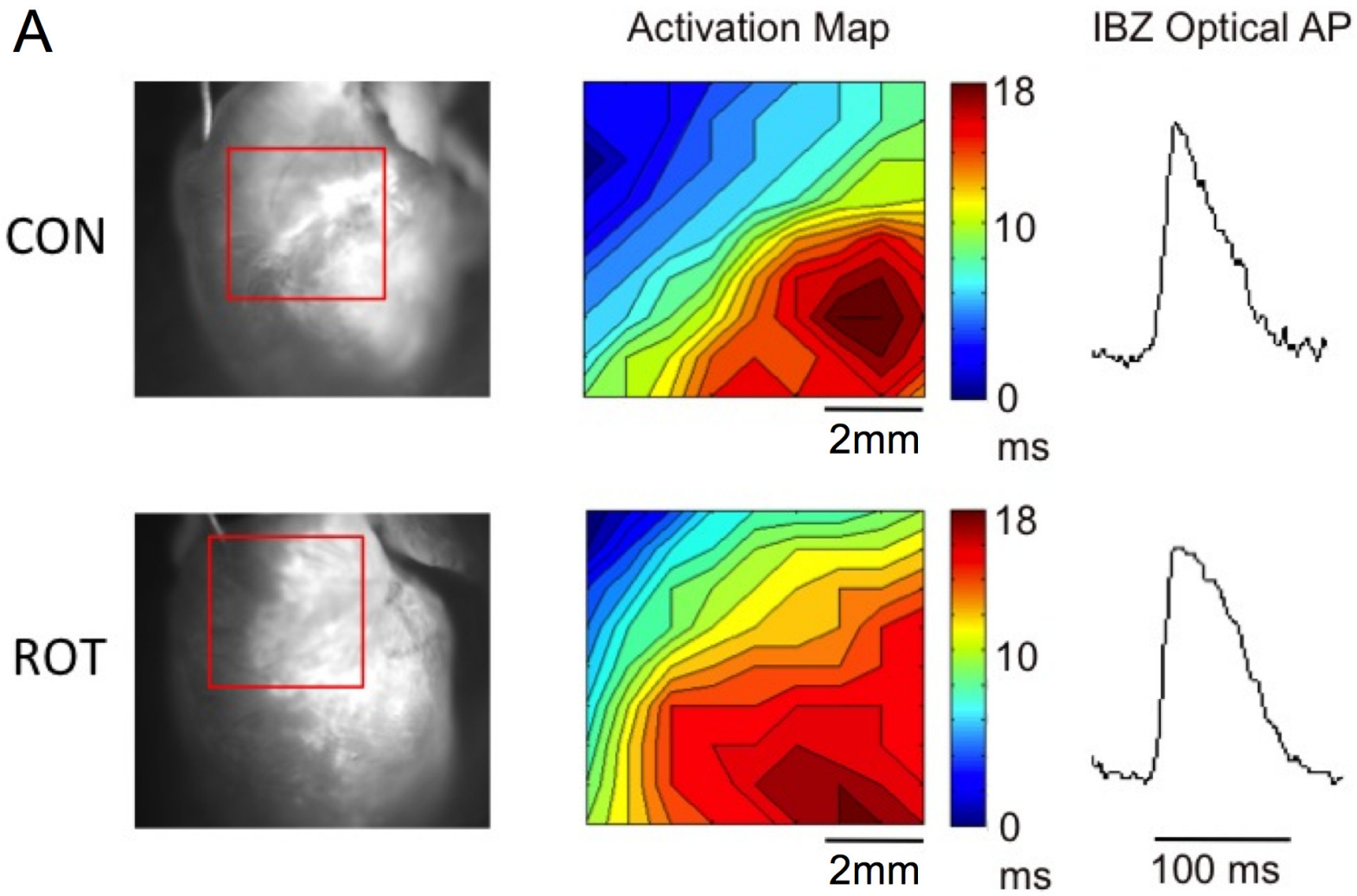
A
Activation Map
IBZ Optical AP
CON
ROT
18
10
0
ms
2mm
2mm
100 ms

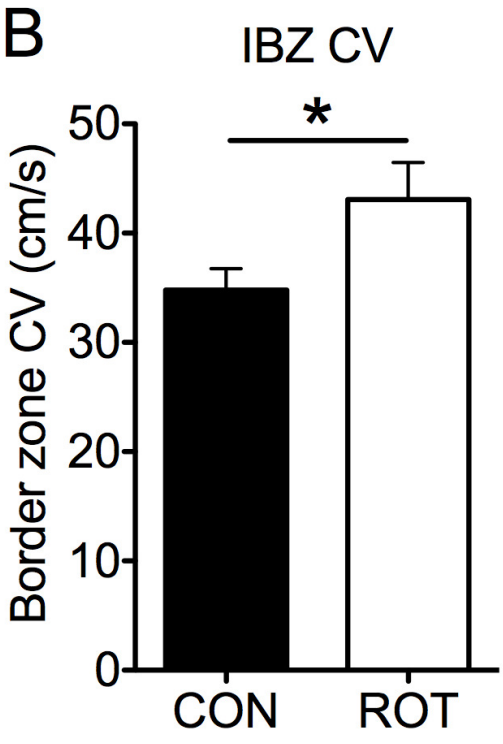
B
IBZ CV
*
Border zone CV (cm/s)
50
40
30
20
10
0
CON
ROT

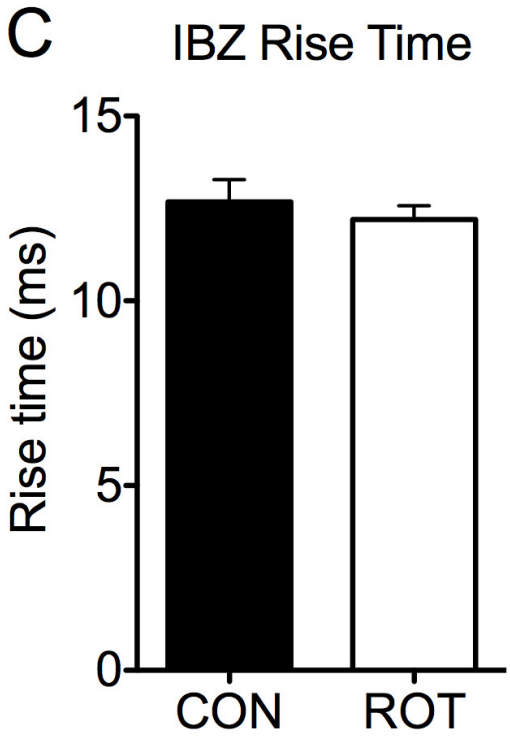
C
IBZ Rise Time
Rise time (ms)
15
10
5
0
CON
ROT

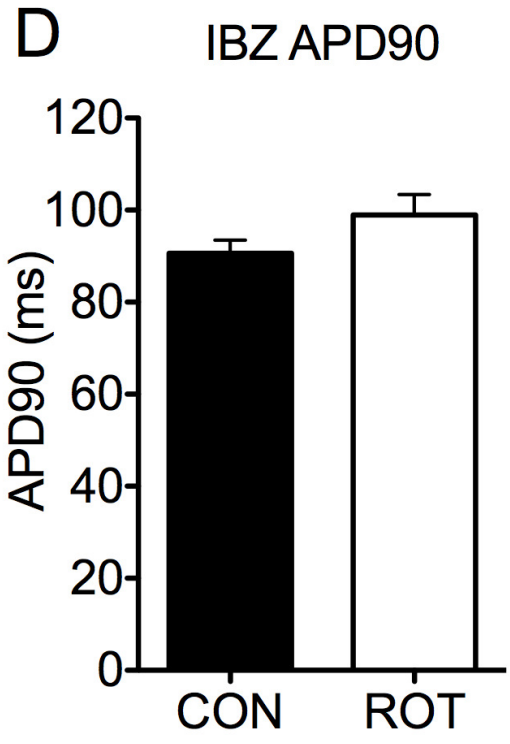
D
IBZ APD90
APD90 (ms)
120
100
80
60
40
20
0
CON
ROT

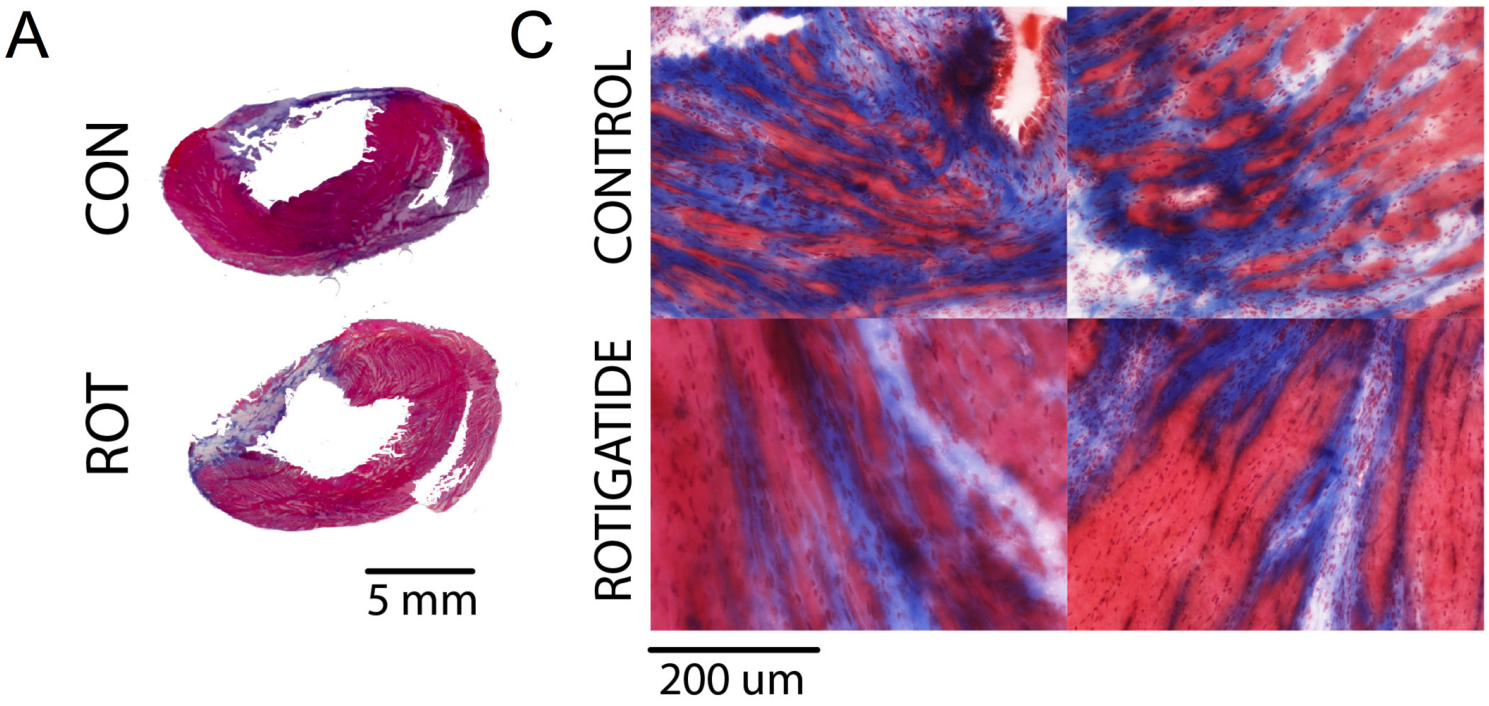
A
CON
ROT
5 mm
C
CONTROL
ROTIGATIDE
200 um

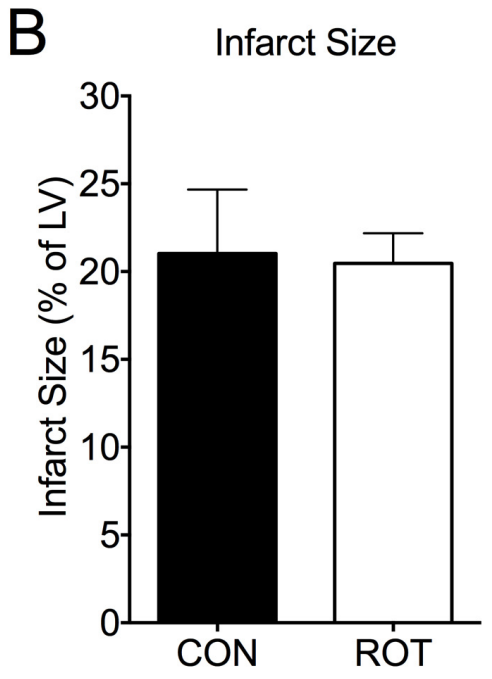
B
Infarct Size
Infarct Size (% of LV)
30
25
20
15
10
5
0
CON
ROT

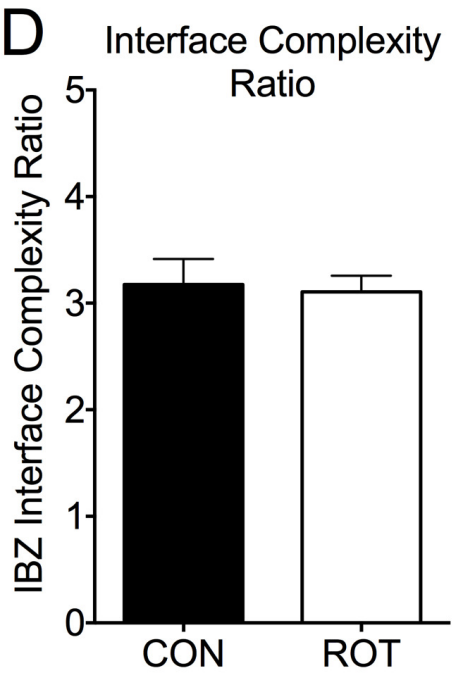
D
Interface Complexity Ratio
IBZ Interface Complexity Ratio
5
4
3
2
1
0
CON
ROT

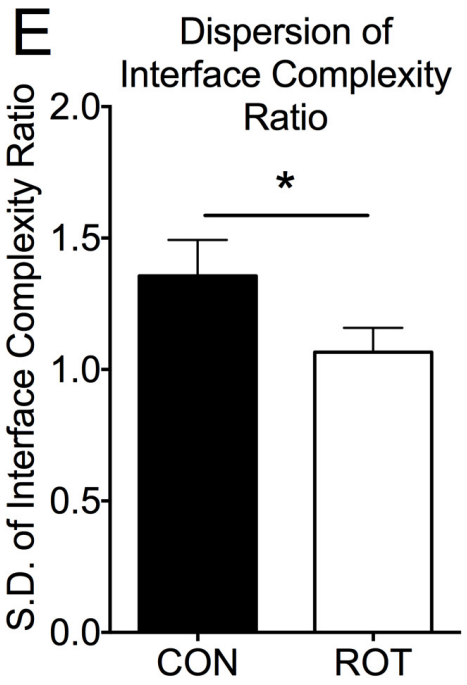
E
Dispersion of Interface Complexity Ratio
S.D. of Interface Complexity Ratio
2.0
1.5
1.0
0.5
0.0
*
CON
ROT

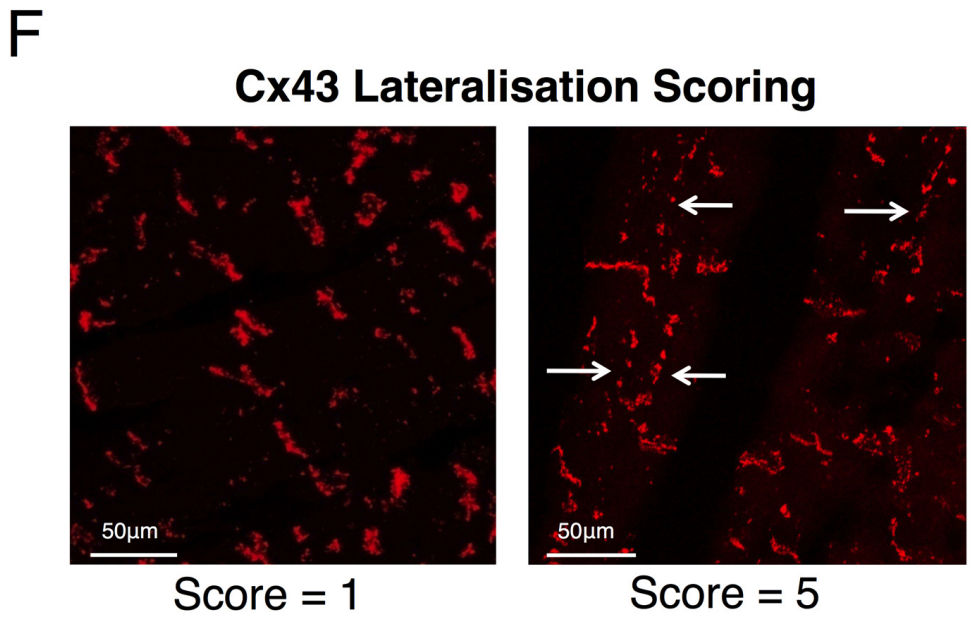
F
Cx43 Lateralisation Scoring
50µm
50µm
Score = 1
Score = 5

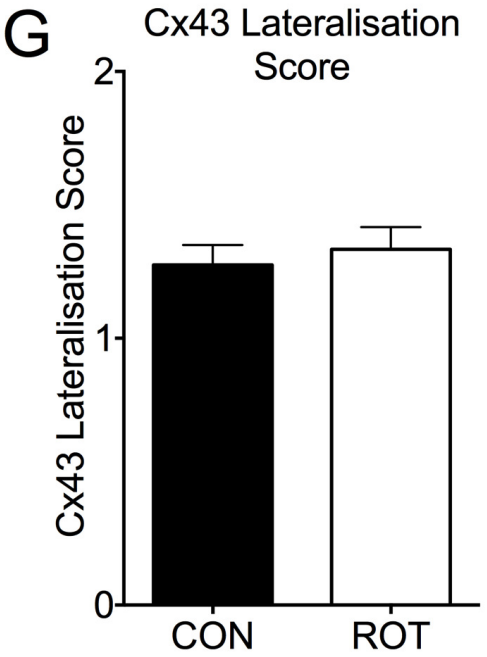
G
Cx43 Lateralisation Score
Cx43 Lateralisation Score
2
1
0
CON
ROT